Multilayer transparent electrodes for flexible and inverted-geometry OLEDs

Seunghyup Yoo*, Chang-Hun Yun, Jae-Woo Park, and Hyun-Su Cho
[1]Dept. of Electrical Engineering, KAIST, Daejeon 305-701, Korea
TEL:82-42-350-3483, e-mail: syoo@ee.kaist.ac.kr.

Keywords : transparent electrode, flexible OLED, inverted OLED, multilayer electrode

Abstract

Multilayer transparent electrodes (MTE) based on an ultrathin metal layer assisted by additional dielectric or semiconducting layers are investigated as electrodes in OLEDs including an inverted geometry. A special attention is paid to their tuning capability in injection behavior and to their potential for ultra-flexible electrodes.

1. Introduction

Since the invention of OLEDs, the choice of transparent electrode for OLEDs has been unarguably indium tin oxide (ITO) films. The recent price hike of ITO films due to an indium shortage resulting from a rapid growth of flat-panel display (FPD) industry, however, has led researchers worldwide to look for transparent electrode technologies which can eventually replace ITO films [1]. In addition, a growing interest for flexible displays is demanding an ultraflexible electrode that would not fail even after repeated number of bending over a small radius of curvature. From the point of view of flexible displays, replacement of ITO electrodes is no longer an option because the integrity of ITO films is known to be severely degraded upon bending [2]. Conducting polymers and carbon nanotube (CNT) films are being explored as transparent flexible electrodes, but their application to OLEDs remains challenging due to their low intrinsic conductivity. Alternative method is to use thin metal films sandwiched between dielectric or semiconducting films in multilayer geometry. While thin metal film by itself can absorb significant portion of incoming light, such multilayer structure can enhance optical transmission by utilizing interference phenomena as in anti-reflection or high-reflection coatings. In this work, we investigate the multilayer electrodes (MTE) consisting of dielectric/metal/dielectric (DMD) layers [3,4] as alternative electrodes for OLEDs including inverted OLED geometry. In addition, the flexibility of DMD-type MTE is also explored from the perspectives of flexible OLEDs.

2. Experimental

Multilayer electrodes were prepared by thermal evaporation using DOV HS-100 system. In case OLED devices were built upon MTE, organic layers and top metal electrodes were deposited without breaking the vacuum to minimize any contamination, unless noted otherwise. When it is necessary to break the vacuum due to the limited number of deposition sources, etc., organic layers did not get exposed to ambient air, because the deposition chamber is integrated with a nitrogen-filled glove box. All the device characterization was done also in the glove box. Current-voltage (*I*-*V*) characteristics and sheet-resistance measurement were recorded using Keitheley 2400 source-measure unit in a 4-wire connection mode. Optical spectrum was measured using the pre-calibrated Stellarnet fiber-optic spectrometer (EPP-2000-UV-VIS-NIR), and luminance-voltage (*L*-*V*) characteristics were measured using the photodiode (Thorlabs, FDS100-cal) with the calibrated spectral response. For characterization of flexibility, several cylindrical objects with various radii of curvature were employed to measure the change in the sheet resistance as a function of radius of curvature. Optical constants used in calculating optical transmission were borrowed from literature [3] or from SOPRA database [5].

3. Results and discussion

Figure 1 shows the optical transmission of MTE based on glass / ZnS(40nm) / Ag(10nm) / ZnS (60nm) layers. It can be clearly seen that the optical transmission of a single Ag film, which is only 30% at a wavelength of 550 nm, can be greatly enhanced to 84% upon use of DMD structure.

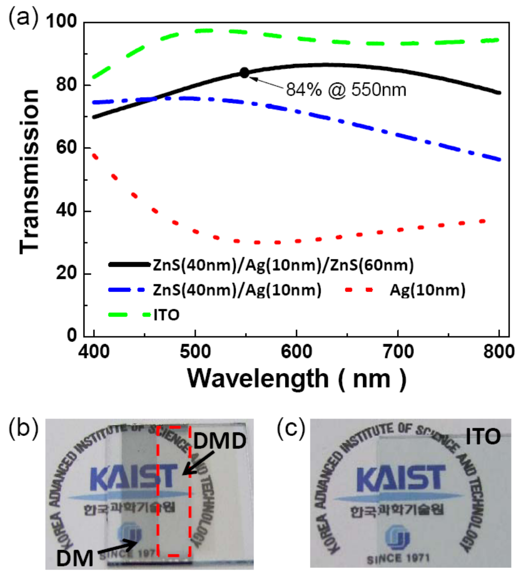

Fig. 1. (a) Transmission of DMD-type multilayer electrodes (MTE) based on glass / ZnS (40nm) / Ag (10nm) / ZnS (60nm). (b) Photograph showing the difference in transparency of MTE with and without the final ZnS layer. (c) Photograph of ITO glass. Transmission in (a) is measured with reference to a bare glass substrate.

Transmission of such multilayer structures can be analyzed using so-called transfer matrix formalism [6], and overall device geometry can be optimized so that the net transmission may be maximized. Figure 2 shows such example for DMD thickness optimization for Ag thickness of 12nm. It can be seen that the optical transmission as high as 89% can be achieved at a configuration of glass/ ZnS(53nm)/ Ag(12nm)/ ZnS (42nm).

Figure 3 shows the *I-V* and *L-V* characteristics of the inverted OLED devices having the structure of glass/X/Alq3 (40nm)/ NPB (30 nm) /WO3(5nm)/Al in bottom emission with X being ITO(170nm) /Ca(1nm) or ZnS(40nm)/Ag(10nm)/ZnS(40nm). While the latter works fine as a cathode, it can be seen that the turn-on voltage gets increased to 9.7 V from 6.2 V for the former. It is noted that ZnS/Ag/ZnS

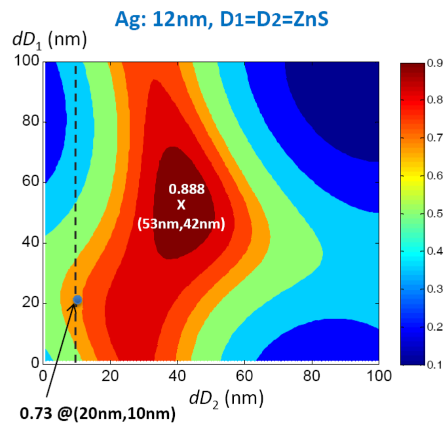

Figure 2. Example of thickness optimization in DMD-type multilayer electrodes where D=ZnS with varying thickness and M=Ag with a fixed thickness of 12nm.

MTE was previously employed in a non-inverted geometry by Pang et al. as anodes replacing ITO [4]. In that previous report, the turn-on voltage was shifted to approximately 12.5V from 4.8 V of the ITO-based reference device. Such large voltage shift is regarded to result mainly from the large injection barrier from Ag to the valence band of ZnS (~6.7 eV). The smaller turn-on shift reported here indicates that the current DMD structure is suited better for inverted OLED geometry because, in this case, the conduction band edge of ZnS (~3.0 eV) is closer to the work function of Ag (~4.5 eV).

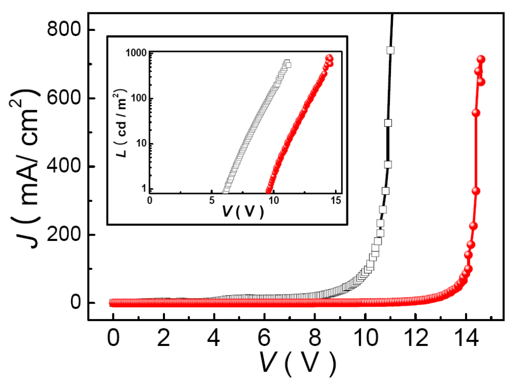

Figure 3. Inverted OLED characteristics with the structure of glass/ X /Alq$_3$ (40nm)/ NPB (30 nm) /WO$_3$(5nm)/Al. X=ZnS (40nm) /Ag(10nm) /ZnS(40nm) (circles) or ITO(170nm)/Ca(1nm) (squares)

We have also looked at the modified MTE structure as anodes in which internal dielectric/semiconducting layer that makes a contact with organic layer is replaced by 5-nm-thick tungsten oxide (WO_3), which is known to make a good hole injection layer to organic hole-transport layer. Replacing the inner ZnS with a thinner WO_3 layer which has a lower refractive index (~1.6) resulted in a decrease in transmission down to 56%. Nevertheless, it can be seen from Fig. 4 that the performance of OLED based on ZnS(40nm)/Ag(15nm)/WO_3(5nm) device is quite comparable to that of the ITO-based reference device.

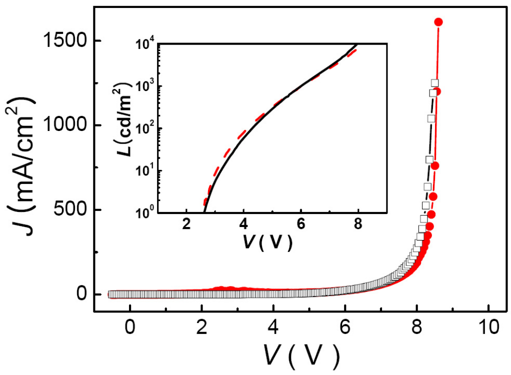

Figure 4. OLED characteristics with the structure of glass/ X / NPB (50nm)/ Alq_3 (50nm)/ LiF(1nm)/ Al. X=ZnS(40nm)/Ag (15nm)/WO_3 (5nm) (circles) or ITO (squares).

Finally, we have explored the DMD MTE as ultraflexible electrodes. Figure 5 compares the sheet resistance of ITO and MTE based on ZnS/Ag after being bent 50 times at a given radius of curvature. While the ITO electrode degrades severely upon bending, the DMD electrode exhibits virtually no degradation even at a radius of curvature as small as 5mm.

4. Summary

We showed that hybrid multilayer electrodes based on dielectric/metal/dielectric (DMD) structures can become versatile transparent electrodes in both inverted and non-inverted geometry. Moreover, it was shown that DMD electrodes can be an excellent candidate for flexible devices in which ITO electrodes are subject to severe degradation.

This work was supported by the ERC program of the Korea Science and Engineering Foundation (KOSEF) grant funded by the Korea Ministry of Education, Science and Technology (MEST) (No. R11-2007-045-01001-0).

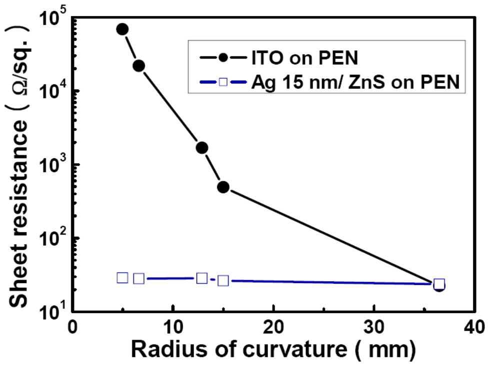

Figure 5. Sheet resistance of ITO films (closed circled) and ZnS(40nm)/Ag(15nm) films (open squares) on PEN substrates after bending 50 times over various radii of curvature.

5. References

1. A. Chipman, *Nature,* **449[7159]**, 131 (2007).
2. G.-F. Wang, X.-M. Tao, and R.-X. Wang, Nanotech. . **19[14]**,145201 (2008).
3. H. Pang, Y. Yuan, Y. Zhou, J. Lian, L. Cao, J. Zhang, and X. Zhou, *Thin Sol. Films* **441**, 200 (2003).
4. H. Pang, Y. Yuan. Y. Zhou, J. Lian, L. Cao, J. Zhang, and X. Zhou, *J. Luminescence* **122-123**, 587 (2007).
5. SOPRA database of optical constants can be downloaded from http://www.sopra-sa.com .
6. L.A.A. Pettersson, L.S.Roman, and O. Inganas, J. *Appl. Phys.* **86**, 487 (1999).